A NUMERICAL INVESTIGATION OF THE TURBULENT BOUNDARY LAYER OVER A ROTATING DISK

Xiaohua Wu
Department of Mechanical Engineering
Stanford University
Stanford, CA 94305-3030, USA

Kyle D. Squires
Department of Mechanical and Aerospace Engineering
Arizona State University
Tempe, Arizona 85287-6106, USA

ABSTRACT

Large eddy simulation (LES) has been used to predict the statistically three-dimensional turbulent boundary layer (3DTBL) over a rotating disk. LES predictions are compared to the experimental measurements of Littell & Eaton (1994), obtained at a momentum thickness Reynolds number of 2660. Predictions of the mean velocities and second-order statistics are in good agreement with data. Conditionally-averaged velocities provide new evidence in support of the structural model of Littell & Eaton (1994) concerning the interaction of mean-flow three-dimensionality and shear-stress producing structures. Inside the buffer region under strong ejections, the conditionally-averaged crossflow (radial) velocity is larger than the unconditioned mean, and the profile conditioned on strong sweeps is smaller than the mean. This is consistent with the notion that streamwise vortices having the same sign as the mean streamwise vorticity, and beneath the peak crossflow location, are mostly responsible for strong sweep events; streamwise vortices with opposite sign as the mean streamwise vorticity promote strong ejections.

INTRODUCTION AND BACKGROUND

Compared to its laminar and transitional counterparts, the fully turbulent three-dimensional boundary layer over a rotating disk has been the subject of relatively few investigations (Figure 1). Unlike 3DTBLs which are formed by turning, via a spanwise pressure gradient or shearing force, an initially two-dimensional turbulent flow, the disk boundary layer is unique in that it is three-dimensional from its inception. Consequently, the underlying structure does not result from perturbing an initially two-dimensional flow, but is inherent to a boundary layer with a continuously applied crossflow. The disk boundary layer is then one of the most canonical platforms for investigation of the underlying structure of 3DTBLs. Increased knowledge and an improved understanding of the disk boundary layer structure establishes an important basis for understanding other 3DTBLs arising in more complex configurations.

The most thorough experimental investigation of the statistical and structural features of the 3DTBL over a rotating disk is that conducted by Littell & Eaton (1994). A key feature of their study concerned modification of boundary layer turbulence by the crossflow. By assuming that the underlying structure of an equilibrium 3DTBL is not fundamentally different from its two dimensional counterpart, Littell & Eaton first hypothesized that the model of Robinson (1991) developed for two-dimensional boundary layers can be used as an approximation to the shear-stress producing structure in their 3DTBL (Figure 2a). In Robinson's model most ejections are found on the upstream side of transverse vortices, which often form 'head' elements of one- or two-sided vortical arches; strong sweeps occur primarily on the outboard side of tilted necks. Using this baseline model, Littell & Eaton (1994) then proposed that the modification of shear-stress producing structure by mean-flow three-dimensionality can be described as follows: the crossflow reduces the ability of streamwise vortices of one sign to produce strong ejections, while weakening the ability of those of the other sign to produce strong sweeps (Figure 2b). In support of their proposition, Littell & Eaton (1994) showed that conditionally sampled wall-normal velocities at $z^+ > 100$, a position above the location of the peak crossflow, exhibited an asymmetry on the upstream and downstream side (in the radial direction) of ejection/sweep events (see also Eaton 1995, Wu & Squires 1997). While this proposition represents a significant step forward in the understanding of 3DTBL structure, a direct test of their model requires examination of the radial velocity profiles beneath the peak of the mean crossflow and conditionally averaged on strong ejections and sweeps. One of the main goals of the present work is to more closely scrutinize the proposed struc-

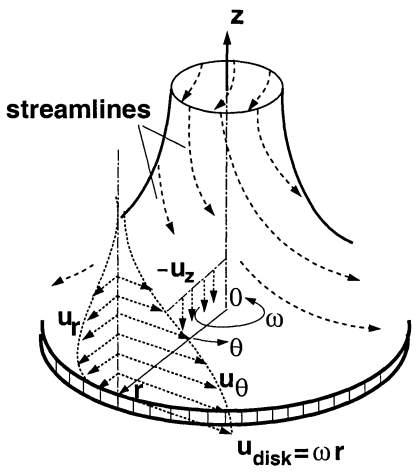

Figure 1: Schematic of the 3DTBL created over a rotating disk in the laboratory coordinate system.

tural model and associated hypothesis advanced by Littell & Eaton (1994) and, in general, to provide a more developed understanding of the similarities and differences between a well-defined, equilibrium 3DTBL over a rotating disk and canonical two-dimensional turbulent flows which have been more widely studied.

Aside from its relevance as a canonical flow for investigating boundary layer structure, successful prediction of the disk flow establishes an important baseline for methods used to predict other complex flows. In fact, noting that few turbulence simulations are available of the disk boundary layer, Johnston & Flack (1996) concluded their review by "urging modellers to tackle this case as a prelude to the prediction of more complex flows". The first objective of the current contribution is accurate prediction of the 3DTBL over a rotating disk and evaluation of simulation results using the measurements of Littell & Eaton (1994).

The numerical approach used in this work is based on large eddy simulation (LES). As described in the next section, LES is used to resolve boundary layer turbulence in a Reynolds number range for which measurements exist, outside the range at which a direct simulation could be considered feasible. While LES permits an accurate description of the disk flow, a time-dependent and three-dimensional simulation poses significant new challenges and calculations of the disk boundary layer must be carefully constructed and performed. In LES a subgrid model is employed to parameterize stresses not resolved by the computational grid. The additional empiricism introduced by the subgrid model must be carefully considered before the results from an LES calculation may be used to gain insight into fundamental aspects of the flow. In addition, a reasonably large body of literature now exists concerning application of LES to prediction of complex turbulent flows. It is clear that comparison to experimental measurements is crucial in order to validate the entire computational approach. The two primary aims of this work are: (1) prediction of the 3DTBL over a rotating disk using LES, and (2) investigation of the underlying structure of the flow. The data of Littell & Eaton (1994) acquired at a momentum thickness Reynolds number 2660 are used to evaluate LES predictions.

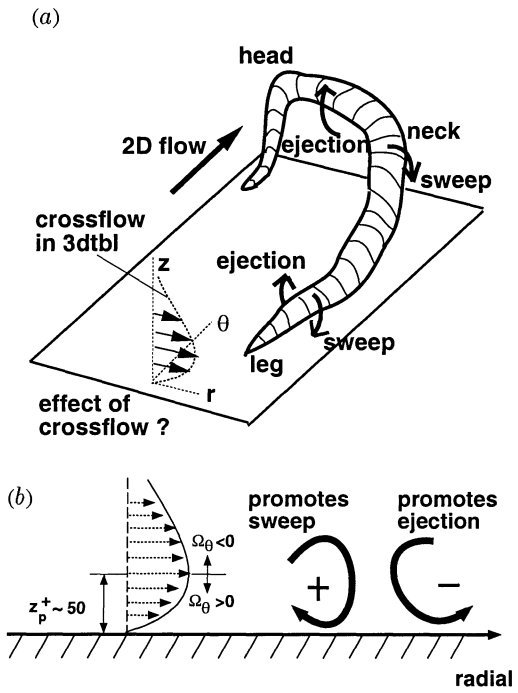

Figure 2: (*a*) Schematic of the canonical 2DTBL structure model of Robinson (1991) and the crossflow profile in the disk boundary layer; (*b*) Littell & Eaton (1994) model of alteration of shear-stress producing events by the mean crossflow (see also Eaton 1995).

SIMULATION OVERVIEW

In this study the SGS stress, τ_{ij}, is modeled as,

$$\tau_{ij} - \frac{\delta_{ij}}{3}\tau_{kk} = \mathcal{L}^m_{ij} - \frac{\delta_{ij}}{3}\mathcal{L}^m_{kk} - 2\nu_T\overline{S}_{ij}\,, \qquad (1)$$

where the modified Leonard term is $\mathcal{L}^m_{ij} = \overline{\overline{u}_i\overline{u}_j} - \overline{u}_i\overline{u}_j$ and an eddy viscosity hypothesis has been used to model the modified cross and Reynolds stresses where ν_T is the SGS eddy viscosity. Three subgrid models are considered: the dynamic eddy viscosity model of Germano *et al.* (1991), the dynamic mixed model of Zang *et al.* (1993), and the dynamic mixed model of Vreman *et al.* (1994). These three closures can be uniformly expressed as,

$$\nu_T = C\overline{\Delta}^2|\overline{S}|\,, \qquad (2)$$

$$C = -\frac{1}{2}\frac{\langle(L_{ij} - H_{ij})M_{ij}\rangle_\theta}{\langle M_{ij}M_{ij}\rangle_\theta}\,, \qquad (3)$$

where

$$M_{ij} = \widehat{\overline{\Delta}}^2|\widehat{\overline{S}}|\widehat{\overline{S}}_{ij} - \overline{\Delta}^2\widehat{|\overline{S}|\overline{S}_{ij}}\,, \qquad (4)$$

$$L_{ij} = \widehat{\overline{u}_i\overline{u}_j} - \widehat{\overline{u}}_i\widehat{\overline{u}}_j\,. \qquad (5)$$

Filtering operations at the test level in the dynamic procedure are denoted using $\widehat{\cdot}$. The large-scale strain rate tensor is S_{ij} and $|\overline{S}| = (2\overline{S}_{ij}\overline{S}_{ij})^{1/2}$. The form of H_{ij} in the mixed models is either from Zang *et al.* (1993) or Vreman *et al.* (1994) (see Horiuti 1997 for additional discussion). Note that when the dynamic eddy viscosity model is used instead of the mixed models, $\mathcal{L}_{ij}^m$ is not explicitly computed, but rather presumed to be closed using the eddy viscosity part of the model.

Filtering was applied in the tangential and radial directions and the grid-filter width was assumed to be equal to the grid spacing in these directions. The test-filter width, $\widehat{\overline{\Delta}}$, was twice the grid-filter width, $\overline{\Delta}$. A top-hat filter was used at the test-filter level, numerical integration as required for the filtering operations was performed using Simpson's rule. A clipping function was used to ensure non-negative of values of C following the streamwise averaging applied to (3), where $\langle\cdot\rangle_\theta$ indicates an average taken in the tangential direction.

The interest of the present investigation is in the fully turbulent disk flow at $Re = 6.5 \times 10^5$ ($Re_{\delta_2} = 2660$). At this Reynolds number, it would be difficult to incorporate into the calculation the region of laminar-to-turbulent transition. It is therefore assumed that the residual effect of transition on turbulence statistics and structure is negligible. Support for this assumption can be found in the work of Lingwood (1996) on the stability characteristics of the disk flow boundary layer. Lingwood's work suggests that transition to turbulence occurs by an absolute instability, and thus the final state determined by nonlinear effects will be relatively independent of the transition process.

The LES equations are solved over a portion of the disk surface, between two radial planes and over a statistically homogeneous tangential dimension. While periodic boundary conditions are applicable in the streamwise (tangential) direction, time-dependent turbulent velocities must be specified at the two radial planes. A method for prescribing turbulent inflow/outflow conditions was developed by taking advantage of the weak dependence of boundary layer length scales with the radial coordinate. The basic method is described in detail in Lund *et al.* (1998). Slight modifications were required in order to apply the technique to the disk. Along the upper surface of the computational domain the normal derivatives of the radial and tangential velocities were prescribed as zero. The entrainment velocity towards the disk surface was specified to satisfy global mass conservation. No slip boundary conditions are applied at the disk surface $z = 0$.

The LES equations were integrated using a fractional step method in cylindrical coordinates (e.g., see Akselvoll & Moin 1996). Second-order accurate central differences were used for approximation of spatial derivatives on a staggered grid, together with a mixed explicit/implicit time advancement of the discretized equations. The continuity constraint was enforced by solving the Poisson equation for pressure using fast transforms along the homogeneous streamwise direction together with successive line over relaxation in the other two inhomogeneous directions. Prior to prediction of the turbulent boundary layer, simulations were first performed in the laminar regime to validate the overall computational approach against the similarity solution. Calculations were performed at two Reynolds numbers in which the flow was initially quiescent. Though not shown here, agreement with the similarity solution in the laminar regime is excellent.

LES calculations of the 3DTBL were then performed at $Re = 6.5 \times 10^5$ corresponding to a momentum thickness Reynolds number $Re_{\delta_2} = 2660$. The height of the computational domain was $23\delta_2$ measured from the disk surface ($z = 0$), where δ_2 is the turbulent boundary layer momentum thickness. The tangential and radial dimensions of the computational domain were $138\delta_2$ and $23\delta_2$, respectively. Uniform grid spacings were applied in the tangential and radial directions, and tanh stretching is used to cluster points near the wall. At $Re_{\delta_2} = 2660$ one viscous time scale ν/u^{*2} is equivalent to 0.2 inertial time units, $\delta_2/\omega r$. From the initial instant, the governing equations for the large-scale field were integrated to steady state at a time step about one viscous time scale. Statistically steady state was reached after about 5200 inertial time units. Results were then sampled over a period of another 2600 inertial time units. Most of the results discussed below are presented in a rotating coordinate system. Velocities in the rotating coordinates (radial, tangential, and wall-normal) are related to their counterparts in the laboratory system via $v_r = -u_r$, $v_\theta = \omega r - u_\theta$, and $v_z = u_z$.

RESULTS AND DISCUSSION

Statistical Features

Calculations were performed to investigate both the effect of grid resolution and role of the subgrid model. Results illustrating the effect of the SGS model are shown in this section. The grid resolution for all cases in the LES predictions presented below was $65 \times 129 \times 75$ in the radial, tangential, and wall-normal directions, respectively. The corresponding resolution in wall units is $\Delta r^+ = 41$, $(r\Delta\theta)^+ = 126$, and $\Delta z^+_{min} = 1$. The calculations are identified as Case 1 (eddy viscosity model of Germano *et al.* 1991), Case 2 (mixed model of Zang *et al.* 1993), Case 3 (mixed model of Vreman *et al.* 1994), and Case 4 (no subgrid model).

Representative results illustrating the overall effect of the SGS model on the mean flow and the turbulent shear stress are shown in Figure 3. The dependent variables are normalized by the disk velocity ωr. The wall-normal coordinate is normalized by the momentum thickness δ_2 based on $0.99\omega r$. Mean flow and turbulence statistics were obtained through averaging over time as well as along the homogeneous streamwise (tangential) direction. Since the momentum thickness Reynolds number Re_{δ_2} varies only 4% along the radial direction from 2610 to 2710, the statistics have a much weaker dependence on the radial coordinate after being normalized by the local disk velocity or local friction velocity (Littell & Eaton 1994). The results shown Figure 3 and in subsequent figures are the averaged profiles for $2610 < Re_{\delta_2} < 2710$.

Figure 3a shows that near the wall, the no-model calculation (Case 4) over-predicts the mean streamwise velocity. Case 2 using the mixed model of Zang *et al.* (1993) yields similar over-predictions as the Case 4 results. Case 1 and Case 3 predictions of the mean streamwise velocity are in good agreement with the data throughout the boundary layer. The largest discrepancy in the mean tangential velocity occurs in the logarithmic region with a maximum error less than 4%

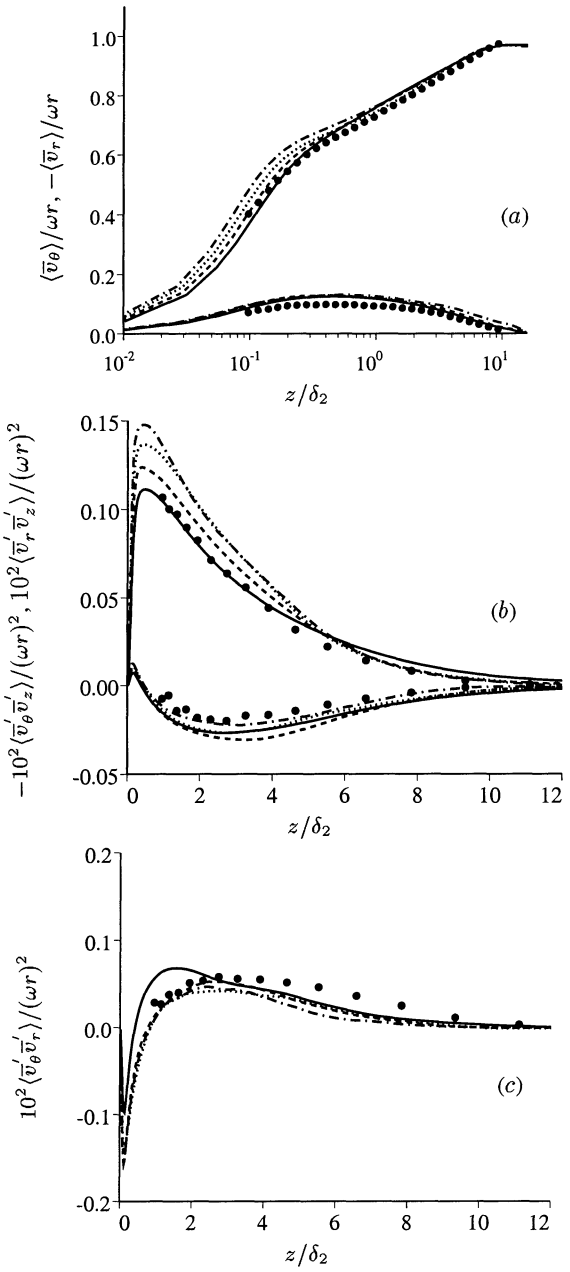

Figure 3: Comparison of LES predictions with experimental measurements. LES: ——— Case 1, ····· Case 2, - - - - Case 3, —·— Case 4; • Littell & Eaton (1994).

of the disk velocity. The predicted mean radial velocity has a peak value of $0.12\omega r$ located at $z^+ = 50$, compared to the peak location $z^+ = 47$ in the experiments of Littell & Eaton. The maximum error in the mean radial velocity occurs near the location of the peak crossflow with a magnitude less than $0.02\omega r$. Also apparent from Figure 3a is that the predicted mean radial velocity is relatively insensitive to the SGS model.

Other boundary layer parameters such as the shape factor and friction velocity agree well with Littell & Eaton (1994), e.g., less than a 2% difference in the friction velocity. The skewing angle made by the wall shear stress with respect to the freestream is about 16° at $Re_{\delta_2} = 2660$, compared to a skewing of 39.6° in the laminar flow.

Predictions of the primary turbulent shear stress $-\langle\overline{v}_\theta'\overline{v}_z'\rangle$ and the secondary shear stress $\langle\overline{v}_r'\overline{v}_z'\rangle$ are shown in Figure 3b. These two stresses appear in the Reynolds-averaged boundary layer equations and the vector formed by $-\langle\overline{v}_\theta'\overline{v}_z'\rangle$ and $\langle\overline{v}_r'\overline{v}_z'\rangle$ is parallel to the disk surface. Note the predicted turbulent shear stresses include the resolved large-scale fluctuations and the subgrid-scale contributions τ_{ij}. The secondary shear stress $\langle\overline{v}_r'\overline{v}_z'\rangle$, although negative through most of the boundary layer, changes sign very close to the disk surface and reaches a minor positive peak. This is consistent with the conjecture made by Littell & Eaton (1994) that $\langle\overline{v}_r'\overline{v}_z'\rangle$ must change sign close to the wall in order to approach the radial wall shear stress. Though not shown here, for the primary shear stress, the peak of the resolved-only profile is 20% lower than the peak in the profile which includes contributions from all the three sources, i.e., the resolved, modeled, and modified Leonard term contributions. Similar to the no-model results, Case 2 predictions are also over the data, analogous to the behavior observed in the mean flow. These profiles agree qualitatively with those reported by Vreman *et al.* (1997) in which a reduced level of SGS dissipation was obtained using the dynamic formulation of Zang *et al.* (1993), resulting in predictions similar to those from simulations using no subgrid model. The other secondary shear stress $\langle\overline{v}_\theta'\overline{v}_r'\rangle$ is shown in Figure 3c. This component does not appear in the boundary layer equation and is usually neglected in 3DTBL analysis (e.g., see Spalart 1989, Littell & Eaton 1994, Johnston & Flack 1996). Figure 3c shows the agreement between the LES predictions of $\langle\overline{v}_\theta'\overline{v}_r'\rangle$ and measurements is reasonable.

Though not shown here, differences in normal stress levels with change in SGS model were smaller for the tangential and radial fluctuations than for the wall-normal velocities. In general, LES predictions without a subgrid model over-estimate velocity fluctuation levels, apparent in the primary stress profiles shown in Figure 3b. While the role of the SGS model on the secondary stresses is more complex than in the mean flow and primary shear stress, the overall agreement of the predicted secondary shear stresses with the experimental measurements of Littell & Eaton (1994) is still reasonable.

The predictions shown in Figure 3 are representative, showing that the disk flow has been accurately predicted. Grid resolutions are fine enough such that there is a relatively weak effect of the SGS model on LES predictions. This is consistent with the relatively fine resolution requirements in LES of boundary layers. These results also suggest that the important large-scale fluctuations in the disk boundary layer have been reasonably well resolved. The accuracy of the predictions and relative insensitivity to SGS model in turn provides confidence that the LES database may be used to probe in greater detail statistical and structural features of the flow.

Structural Features

The structural model of Littell & Eaton (1994) is based on the hypothesis that the overall shear-stress producing structure in the disk flow can be modeled as an appropriate alteration of that in a canonical two-dimensional boundary layer, i.e., the arch-like vortex structural model of Robinson (1991). Based on their measurements, Littell & Eaton (1994) proposed that the modification by the crossflow alters the relative strengths of ejections and sweeps arising from structures with different signs of streamwise vorticity. Specifically, their model considers a sub-division of vortical structures into two classes (+ or −) according to the sign of streamwise vortices relative to that of the mean streamwise vorticity (Figure 2). Class + structures are those whose streamwise vortices have the same sign as the mean streamwise vorticity beneath the peak crossflow location. Class − structures refer to those whose streamwise vortices have opposite sign as the mean streamwise vorticity beneath the peak crossflow.

The model is then that Class + vortices are mostly responsible for strong sweep events, while Class − structures promote strong ejections. A consequence of this model is that beneath the location of the peak crossflow, conditionally sampled radial velocities should be smaller than the mean for strong sweep events, and the profile for strong ejections should be larger than the mean (c.f. Figure 2b). In support of this model, Littell & Eaton (1994) used the asymmetry of their conditionally sampled wall-normal fluctuating velocity upstream and downstream (in the radial direction) of shear-stress producing events. A direct examination of the model can be undertaken by measuring the conditionally averaged radial crossflow velocity for shear-stress producing events.

Conditionally-averaged velocities occurring under strong ejection and sweep events are shown in Figure 4. The criteria used in Figure 4 to define strong ejections is $-\overline{v}'_\theta \overline{v}'_z > \beta \overline{v}'_{\theta,rms} \overline{v}'_{z,rms}$ and $\overline{v}'_z > 0$, while the criteria for strong sweeps is $-\overline{v}'_\theta \overline{v}'_z > \beta \overline{v}'_{\theta,rms} \overline{v}'_{z,rms}$ and $\overline{v}'_z < 0$. To check the consistency of the results, two values of β are used, i.e., $\beta = 6$ and 10. Note that since the ratio of shear stress $-\langle \overline{v}'_\theta \overline{v}'_z \rangle$ to the product of the intensities $\overline{v}'_{\theta,rms} \overline{v}'_{z,rms}$ is around 0.5 in the buffer region, these thresholds translate into requiring the instantaneous shear stress be 12 and 20 times the mean primary shear stress, respectively. The streamwise profiles in Figure 4a show the expected and substantial differences between the mean and conditionally-averaged velocities. This is consistent with the consensus discussed in Robinson (1991) that in most cases the variance of the measurable attributes of shear-producing structures about their mean values is very large. Figure 4b shows that beneath the location of the peak crossflow, $z^+ = 50$, the conditionally-averaged radial profile is larger than the unconditioned mean for strong ejection events, and has a deficit compared to the global profile for strong sweeps. There is also an indication that these two profiles intersect slightly above the location of the peak crossflow velocity, in direct support of the model of Littell & Eaton (1994).

Although Figure 4 provides new proof in support of the 3DTBL structural model advanced by Littell & Eaton (1994), these results have not yet touched upon the important hypothesis made in their work, i.e., the arch-like vortex structure discussed in Robinson (1991) comprising the underlying structure of canonical two-dimensional boundary layers can be used as a baseline in the disk 3DTBL. As pointed out by Johnston & Flack (1996), this assumption has been accepted to date more or less as a fact based partly on intuition, partly on single-point statistics, and partly on visualizations which showed that low and high speed streaks in two-dimensional boundary layers are also present in many 3DTBLs. An example from the disk flow is presented in Figure 5, which shows isosurfaces of the instantaneous pressure fluctuation. Only strong negative fluctuations are shown, corresponding to low pressure cores. The figure shows at this particular instant there exists a well-defined arch-like vortex structure in remarkable resemblance to that drawn in Figure 2 for 2DTBLs. Because of the quasi-periodic boundary condition applied in the radial direction, part of the longer leg of the arch-like vortex near the outer boundary is displaced to the inner radius. Figure 5b shows contours of the instantaneous azimuthal velocity fluctuation $\overline{v}'_\theta/\omega r$ at $z^+ = 5$. Apparent in the figure are elongated regions of low- and high-speed fluid. The streaks are not aligned with the azimuthal direction, rather, they are skewed away from the disk center by the crossflow.

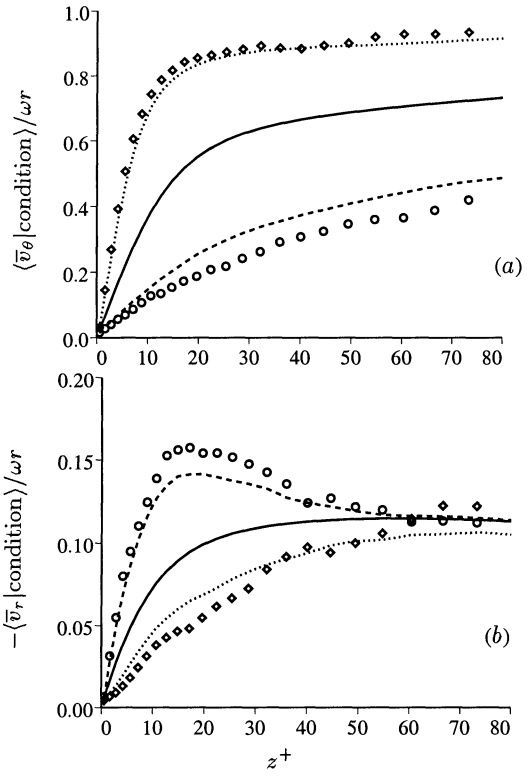

Figure 4: Conditionally averaged velocities. ---- ∘ averaged using the strong ejection condition $-\overline{v}'_\theta \overline{v}'_z > \beta \overline{v}'_{\theta,rms} \overline{v}'_{z,rms}$ and $\overline{v}'_z > 0$; ····· ◇ averaged using the strong sweep condition $-\overline{v}'_\theta \overline{v}'_z > \beta \overline{v}'_{\theta,rms} \overline{v}'_{z,rms}$ and $\overline{v}'_z < 0$; lines: $\beta = 6$; symbols: $\beta = 10$; ——— mean; (*a*) streamwise; (*b*) radial.

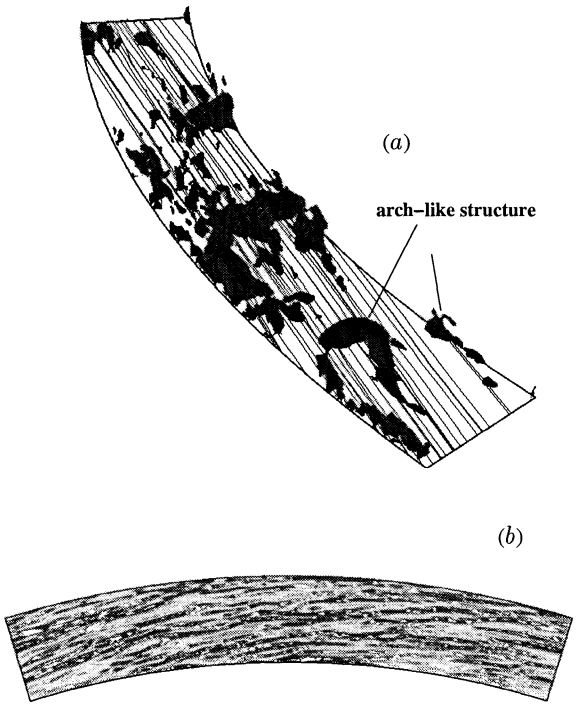

Figure 5: (a) Isosurfaces of instantaneous low pressure cores showing the vortical structure similar to Robinson (1991), also shown are surface streamlines at the same instant. (b) instantaneous azimuthal velocity fluctuations $\overline{v}_\theta'/\omega r$ at $z^+ = 5$.

SUMMARY

These simulations have answered to a satisfactory degree the call by Johnston & Flack (1996) for turbulence modellers to tackle the disk 3DTBL as a prelude to computation of more complex engineering 3DTBLs. Aside from this contribution, one of the more interesting findings are the conditionally averaged velocities obtained for strong ejection/sweep events. These results have offered strong evidence to support the structural model advanced by Littell & Eaton (1994) that streamwise vortices with the same sign as the mean streamwise vorticity are mostly responsible for strong sweep events, streamwise vortices having opposite sign as the mean streamwise vorticity promote strong ejections. Other statistical descriptors of the disk flow not presented here show strong similarities to two-dimensional turbulent boundary layers. This provides some quantitative indirect support to the hypothesis invoked by Littell & Eaton (1994) and Johnston & Flack (1996) that appropriate vortical structural models developed for two-dimensional boundary layers (e.g., by Robinson 1991) may be used in equilibrium 3DTBLs.

The 3DTBL over a rotating disk considered in this work can be classified as a canonical case, representative of equilibrium 3DTBLs, especially those created over infinite geometries and which are three-dimensional from inception. Examples include the Ekman layer and the 3DTBL created by a rotating freestream velocity vector (Spalart 1989). The statistical and structural properties discussed in the present study are expected to apply to other equilibrium 3DTBLs (see also Wu & Squires 1997).

Acknowledgments

This work is supported by the U.S. Office of Naval Research (Grant Numbers N00014-94-1-0047 and N0014-94-1-1053), Program Officer: Dr. L. Patrick Purtell). The authors gratefully acknowledge valuable discussions with Prof. J.K. Eaton and Dr. T.S. Lund. Simulations were performed on the Cray C90 and T90 at the U.S. Department of Defense High Performance Computing Major Shared Resource Centers (CEWES and NAVO).

REFERENCES

Akselvoll, K. & Moin, P., 1996, "Large-eddy simulation of turbulent confined coannular jets", *J. Fluid Mech.*, vol. 315, 387-411.

Eaton, J.K., 1995, "Effects of mean flow three-dimensionality on turbulent boundary-layer structure", *AIAA J.*, vol. 33, pp. 2020-2025.

Germano, M., Piomelli, U., Moin, P. & Cabot, W.H., 1991, "A dynamic subgrid-scale eddy viscosity model", *Phys. Fluids*, vol. 3(7), 1760-1765.

Johnston, J.P. & Flack, K.A., 1996, "Review-advances in three-dimensional turbulent boundary layers with emphasis on the wall-layer regions", *J. Fluids Eng.*, vol. 118, 219-232.

Horiuti, K., 1997, "A new dynamic two-parameter mixed model for large-eddy simulation", *Phys. Fluids*, vol. 9, 3443.

Lingwood, R.L., 1996, "An experimental study of absolute instability of the rotating disk boundary layer flow", *J. Fluid Mech.*, vol. 314, 373-405.

Littell, H.S. & Eaton, J.K., 1994, "Turbulence characteristics of the boundary layer on a rotating disk", *J. Fluid Mech.*, vol. 266, 175-207.

Lund, T.S., Wu, X. & Squires, K.D., 1998, "Generation of turbulent inflow data for spatially-developing boundary layer simulations", *J. Comp. Physics*, vol. 140, 233-258.

Robinson, S.K., 1991, "Coherent motions in the turbulent boundary layer", *Annu. Rev. Fluid Mech.*, vol. 23, pp. 601-639.

Spalart, P., 1989, "Theoretical and numerical study of a three-dimensional turbulent boundary layer", *J. Fluid Mech.*, vol. 205, 319-340.

Wu, X. & Squires, K.D., 1997, "Large eddy simulation of an equilibrium three-dimensional turbulent boundary layer", *AIAA J.*, vol. 35, 67-74.

Vreman, B., Geurts, B. & Kuerten, H., 1994, "On the formulation of the dynamic mixed subgrid-scale model", *Phys. Fluids*, vol. 6(12), 4057-4059.

Vreman, B., Geurts, B. & Kuerten, H., 1997, "Large eddy simulation of the turbulent mixing layer", *J. Fluid Mech.*, vol. 339, 357-390.

Zang, Y., Street, R. & Koseff, J. R., 1993, "A dynamic mixed subgrid-scale model and its application to turbulent recirculating flows", *Phys. Fluids*, vol. 5(12), 3186-3196.